

Author Response to Report #2 Submitted by Anonymous Referee #3 in Support of the Editor's Decision for manuscript # **hess-2018-230** titled:

Mangel et al: Reflection tomography of time-lapse GPR data for studying dynamic unsaturated flow phenomena

To the Editor:

Thank you for all your work in soliciting reviews for our manuscript and managing the submission process. Our response to points made by Anonymous Reviewer #3 are below and placed within the original text for context. Original text from the reviewer is denoted below in *italicized text*, whereas our responses are in regular font.

Overall, the authors strongly disagree with the comments of Reviewer #3. We point to what seems to be a fundamental misrepresentation (and perhaps misunderstanding) of our goals and outcomes by the reviewer. The work presented in this manuscript is the first time that time-lapse monitoring of infiltration has been attempted using GPR reflection tomography. Such work was not possible in the past due to a lack of automated data collection systems that could collect the massive volumes of data required quickly enough to enable the imaging of dynamic events, though there has been a limited history in the literature where reflection tomography has been used to image static spatial variations in water content (as we stated clearly in the manuscript). Now that we have developed an automated GPR system, dynamic imaging has become a possibility and it is of importance to report to the hydrologic (and geophysics) community the feasibility of such an approach. We note that this application of reflection tomography is distinct from static imaging in that water content distributions observed during flow may be significantly different than under static conditions (e.g., due to the possible presence of flow fronts, gradients, instabilities, fast transients, and heterogeneities impacting water content distributions). Thus our goal in this paper is to contribute a baseline understanding of this new monitoring technique for the community by “evaluat[ing] reflection tomography of high-resolution GPR data as a tool for observing and characterizing unsaturated flow patterns during infiltration” (lines 58-59). We perform this evaluation using accepted reflection tomography algorithms that represent the state-of-the-science and we report our findings clearly and directly, i.e., in the manner that is required for the integrity and progress of science, not in a manner that simply has the objective of publishing a “nice result”. To summarize, our manuscript makes the following important contributions:

- (1) this first of its kind study establishes that time-lapse GPR reflection tomography of a dynamic infiltration event is now technically possible, and we set a reference point for future studies;
- (2) we use numerical modeling to establish a baseline for the potential and limitations of time-lapse GPR reflection tomography under idealized conditions – it is not possible for a real-world application to perform better than what is shown in the synthetic study (Figure 3) and the scenarios given provide insight regarding where GPR reflection tomography is likely to fail in practice;
- (3) we provide estimates of the quantitative error to be expected in an imaging scenario utilizing the current state-of-the-science reflection tomography techniques (these errors will obviously decrease in future as new inversion algorithms are developed for dynamic imaging problems); and
- (4) we show that it is possible to achieve an imaging accuracy with real empirical data that is similar to that achieved with the synthetic baseline (i.e., the limitations are in the inversion algorithm, not the data).

We contend that these findings are important outcomes to report to the scientific community as they establish a scientifically sound and robust assessment of this new method's potential and limitations when used in hydrological applications.

Reviewer #3 did not present any evidence in their comments arguing that similar work has been previously reported in the literature or that there are any scientific flaws in our analysis that could potentially be corrected or provide justification for rejection of the manuscript. The fact that the reviewer does not like the results that we reported, which are based on a well-established and technically sound analysis approach that is well-documented in the literature, is neither relevant nor reflective of the scientific method: the results we obtained are what they are and it is our duty to report these results to the community. The fact that the reviewer states that they see value in having our work remain available to the community as a “discussion paper” is clear evidence of their perceived value of the manuscript and contradictory to their recommendation that the paper be rejected.

While we appreciate and agree with the reviewer’s enthusiasm for the potential of GPR to provide additional and deeper insights into unsaturated flow, the arguments laid out by the reviewer below are the framings of a future research program, not critical assessments of our analysis or the results that we have presented. We agree that there are opportunities to develop new algorithms and approaches that could indeed provide improvements over the existing and accepted reflection tomography methodology. These new algorithms do not yet exist, however, and it is therefore completely unreasonable for a reviewer to suggest that our paper should be rejected because we did not use such non-existent analysis strategies, particularly when our work has been based on sound science and has been recognized as a valuable contribution by multiple reviewers.

We are hopeful that the two previous critical reviews, which the authors have addressed, and the current recommendation by a third reviewer to publish the manuscript as-is, are sufficient to justify publication of this manuscript in HESS. We are prepared to make further revisions to the manuscript given guidance, but the review below does not provide actionable items justifying changes at this time. Further responses to each reviewer comment are given below.

The paper under review for publication in HESS by Mangel et al aims at employing a reflection tomography based inversion algorithm, which is well-established for calculating subsurface velocity distributions from CMP GPR measurements in stationary conditions for deriving – by proxy – subsurface water content – distributions. In contrast to previous publications, here the focus is on dynamically changing conditions during infiltration experiments.

First of all, I would like to specifically laud the authors for their dedicated experimental approach and congratulate them for their laboratory setup and the undoubtedly involved data set which may yet hold the key to studying the infiltration experiments they monitored by GPR in so much detail. However, the key question for whether the currently submitted work warrants a dedicated publication is whether the authors found a novel and robust way to extract meaningful and relevant information from this great dataset. Unfortunately, I am convinced that the inversion approach chosen for this publication in its current form falls short of achieving that aim (i.e., as the title states: Usage of this algorithm for “studying dynamic unsaturated flow phenomena”) and does not give justice to the information potentially contained in their elaborated dataset.

The authors appreciate praise in performing the research but argue that the data presented does indeed represent “a novel and robust way to extract meaningful and relevant information” given that currently there are no other methods (geophysical or otherwise) to completely non-invasively monitor water content of soils at this resolution over large areas. If the reviewer feels that there are comparable methods that demonstrate our work does not represent an advance in the field, they should have cited that literature to support their argument. Their failure to do so leaves us unable to respond and we believe this is a result of

the fact that no such prior work that exists in the literature given that ours is a first-of-its-kind study. While we agree with the reviewer that the errors are high compared to what can be achieved with a point sensor (e.g., TDR), there is no comparable baseline for a completely non-invasive dynamic GPR imaging technique such as that obtained here (e.g., Moysey et al. (2004) showed that even borehole-based GPR tomography, which is a much simpler and better constrained problem than that of surface-based reflection tomography, can have errors >10% (vol./vol.) water content simply due to inversion errors and scale).

Furthermore, our goal here was to test and evaluate the existing reflection tomography algorithm and evaluate its performance, not to develop a new algorithm. The “novelty” in this work is in taking a unique dynamic data set, which has until now been unachievable, and combining it with a standard, yet state-of-the-science algorithm for analyzing the data. We welcome the opportunity to share this data set with others through this publication in HESS, which will allow for the development and testing of new algorithms that can be compared against the baseline performance established in this manuscript.

The inversion algorithm's trouble is quite clearly shown already by the simulation based results the authors present in Figure 3: Here, the authors first calculate water content distributions from HYDRUS-2D (figure 3, left column), then derive GPR profiles from these distributions (examples shown in figure 2) and feed these into their tomography algorithm to retrieve the respective water content distributions (figure 3, center column). In the first case, as the authors admit themselves, their algorithm fails completely to capture the velocity profile, since there is simply not enough information for this approach to work with. OK.

Note that we revise figure 3 as a result of a later comment by Reviewer #3, though it does not alter this discussion point. The authors agree that the results presented in figure 3a-c leave much to be desired. We discussed this in the manuscript as stemming from an intrinsic limitation of the information in the data due to a lack of GPR reflectors: only the average water content can be determined because of the limited spatial data coverage near the reflection targets (i.e., at the bottom interface of the model) and this is therefore an intrinsic limitation of the data and not a critical limitation of the algorithm itself (lines 152-156). The goal of the modeling is to demonstrate scenarios highlighting the strengths and weaknesses of the reflection tomography approach. Simply reproducing the water content distribution is unrealistic for any tomographic method and thus we instead aspire to help the reader understand challenges that may be faced in imaging different flow scenarios, i.e., in this case the fact that the lack of reflectors prevents the estimation of vertical water content variability. Furthermore, the authors argue the significance of this result as it directly illustrates one limitation to the approach; if minimal reflectors are present in the data, the tomography results suffer. In general, it is critically important to not only understand where the method succeeds, but also where it fails. Understanding the limitations of any method is crucial to application and deserves just as much attention as more successful results.

It is possible that other algorithms could help to alleviate the limitation of the imaging to some extent. For example, it is possible that more advanced algorithms like full-waveform inversion could make use of reflection amplitudes to better account of the vertical variability, though it is not clear that this is the case given that the fundamental limitation here was the lack of reflection points due to the homogeneity of the subsurface and absence of a target infiltration plume. Full-waveform inversion is still being developed for surface GPR applications, however, and is significantly beyond the scope of this manuscript [Ernst et al. 2007; Meles et al. 2010; Busch et al. 2014; Lavoué et al. 2014]. Even if it were to be found in later studies that full waveform inversion could improve the imaging, it still requires a starting model that would likely be obtained from a reflection tomography approach like that we have presented (lines 211-213).

However, this remains true for the second case – the algorithm basically does not resolve the infiltration plume at all (3d-f).

This statement by the reviewer is demonstrably false as Figure 3f shows an error of only a few percent behind the wetting front. The results also illustrate that the shape of the wetting front can be reconstructed by the tomography algorithm. Comparing Figure 3f to the exact same case with no infiltration front (Figure 3c) clearly demonstrates that the additional information provided by reflections generated by the presence of the wetting front has resulted in new, spatially localized information. We highlighted this in the discussion on lines 157-162. The problem here is that the algorithm struggles in imaging the gradient nature of the capillary fringe present at the base of the model, though this limitation was already clear from the prior scenario. Perhaps the reviewer was misled by the minimal color contrast in figure 3e, which the authors can correct by adjusting the colormap if required. Regardless, no scientific metric is presented in the reviewer's assessment of the results to determine what standard the reconstruction is being held against.

We have corrected one error in the text identified on line 162 of the manuscript where Figure 2g was misidentified as Figure 2e.

In the third case (3g-i), the algorithm actually outputs an infiltration plume - which could be expected since the input in this case is to first order approaching a two-layered system and no longer includes a water table below.

The arguments presented by the reviewer that the system is approaching a simple two-layered system are irrelevant. The advantage of the reflection tomography algorithm over others is that it can account for lateral and vertically variable velocity fields. The same argument for a less complex 'layered system' could be made regarding the model presented in figure 3a-c, yet the tomography algorithm cannot resolve the layered structure in that case. As the authors mention, this is due to limited spatial coverage by the GPR data. Furthermore, the phrasing used here by the reviewer, e.g. 'which could be expected', is not consistent with the reality of tomographic imaging methods which often face spatial resolution, smoothness, and trade-off issues. The results observed are not unexpected and need to be addressed to avoid misinterpretation by future practitioners of GPR reflection tomography.

However, and this is in my opinion crucial if such an approach is supposed to be used for studying infiltration experiments, the algorithm misplaces the position of the infiltration front by about a factor of two (the "true depth" of the plume is about 0.23 m judging from figure 3g, the calculated position clearly surpasses 0.4 m). If the results are aimed at "informing models of hydrologic processes" (L210), adding this information on top of the rather large water content deviations will certainly not be beneficial to the output of any model. From the examples in figure 3, only the very last case (Figure 3 j-l) might be deemed an acceptable result, although the shape of the infiltration front and lateral expansion is still not captured (which would be important information for the hydrological model!). As stated above, this is most likely due to the fact that as the infiltration plume advances into the medium and increases in size, it resembles a much more simple two-layered medium case – again without the presence of a water table.

The reviewer raises a good point here; the 0.10 m error in the depth of the wetting front lacks context within the inversion algorithm. Therefore, the authors have added the following sentence when discussing these results.

“The tomography algorithm overestimates the depth of the wetting front by roughly 0.10 m for the case presented in Figure 3g-i, which is likely due to smoothing effects required to regularize the inversion or an error in the picking of the wetting front horizon.”

To give a better indication of whether this algorithm could - at least based on a numerical study - provide an output, which would be useful for studying the actual hydrologic infiltration process it would be necessary to present a detailed time-lapse assessment of how a progressing infiltration plume can be resolved in the first place. At minimum this could start from a time-lapse representation (e.g., a movie) of results with a good enough temporal resolution: E.g., of the “true” water content calculated by HYDRUS-2D on the left and the tomography result on the right – depicting the temporal evolution of both the infiltration event and the corresponding tomography result for each timestep. This could in principle then be used both for a rigorous error assessment, which is missing so far, and for discriminating periods in time during the infiltration process in which the situation is just too complex for the current tomography approach and where it deliver at least useful information. From the examples shown in the paper, I take it that first, the imaging fails completely, then the infiltration is resolved as being much faster than in reality while in the end a simpler situation is reached in which an acceptable result may be achieved: Hence this looks like there is a point where the inversion actually somehow converges towards reality which should be clearly identified and discussed. Without such an assessment, which does not only encompass comparing average water contents, I do not see much reason for trusting the results of the measurement inversions shown later. In 2019, for studying infiltration processes with GPR, a quantitative “average error of 5-10%” in water content is not enough if not at least the dynamics can be qualitatively resolved much better. In fact, it would be truly a pity if matching average water contents to within 10% would really be all that can be done with your elaborated dataset.

The reviewer misunderstands the goal of the modeling. We do not represent different times during infiltration event, but rather cases designed to illustrate different scenarios of water content distribution that can provide insights in the interpretation of time-lapse data (i.e., no infiltration plume, the influence of a capillary fringe on the imaging, and the case where no diffuse water table is present). Regardless of the fact that we present only a few representative times for the tomographic imaging of the experimental dataset (i.e., before, during and after the infiltration event), we selected these specific times to illustrate that the reflection tomography does indeed show substantial changes in water content that are realistic and generally consistent with measurements made at point probes (at least in trend if not in magnitude due to scale issues between the imaging and point sensors). The reviewer does not demonstrate an understanding of the intensive effort required for inversion of these data sets. The work for this manuscript was performed in a seismic imaging software which is engineered to handle large seismic data sets, similar to those obtained here, and involves substantial manual intervention to identify reflections in the data. Other limitations include the use of Kirchoff migration, which the authors note as a limitation in migrating the data (lines 208-211). We agree that future efforts building on this manuscript should involve the development of algorithms that can facilitate the analysis of massive timelapse datasets like those we can now collect.

Finally, the results we report are not a matter of “trust”. They are the result of direct comparisons between the imaging results and point sensors (or true model for the synthetic data). Such comparisons and the reporting of these results are the foundations upon which science is built and advanced through successive improvements and discoveries over time. Thus the results we report here are required as a foundation upon which future work can be built and compared to demonstrate further advances. It appears that this reviewer does not understand this fundamental premise of science. Instead it appears that the reviewer favors tweaking algorithms to cherry pick “good” results, which we believe to be an increasingly common and dangerous approach to science. We fundamentally reject this philosophy and hope that the editors of HESS agree that such an approach is not an approach that promotes the continued development of strong scientific community.

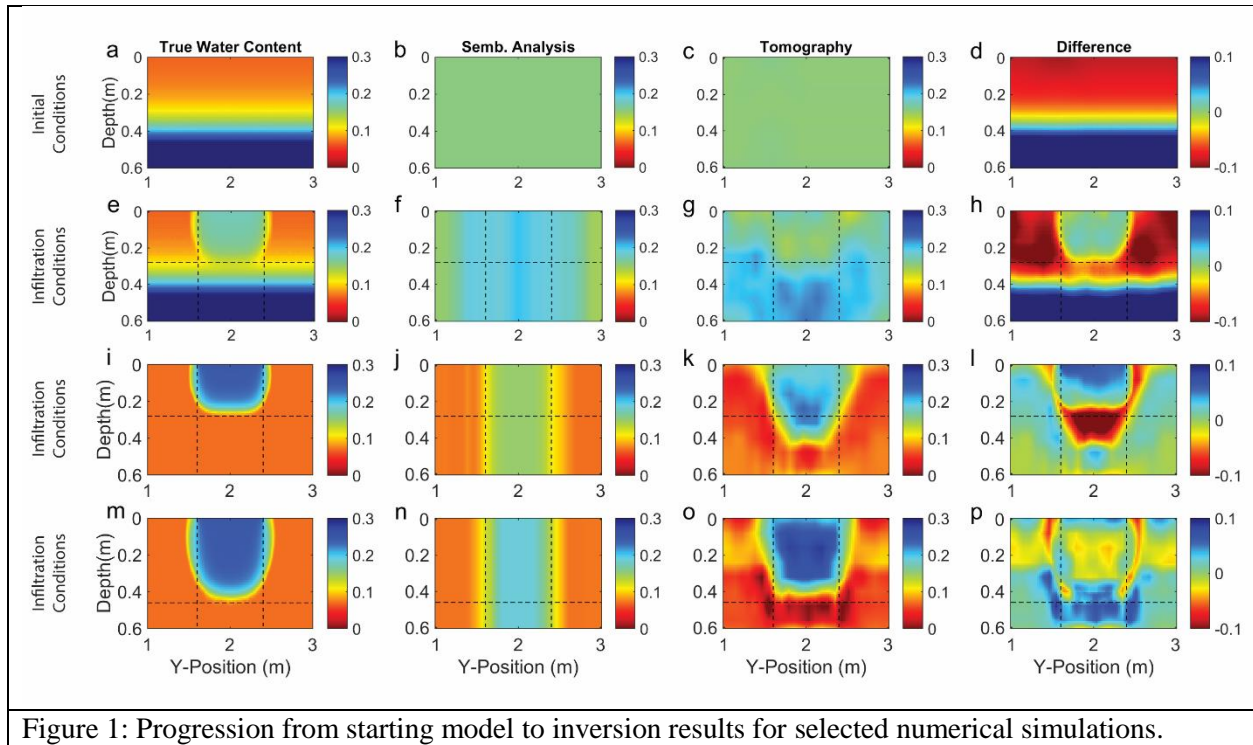
From the work presented here it seems clear that for studying dynamic unsaturated flow phenomena the authors should attempt to leverage much more of the information actually contained in the dataset. Information is already scarce for tomography algorithms based on surface data in stationary conditions. In such a dynamic infiltration experiment context, any viable approach will therefore have to give credit to the specific strengths of such a dataset. Getting more acceptable results may, e.g., include concurrently considering information from the air/groundwave and the wetting front reflection – which would likely not be directly possible in the framework of the present version of the inversion algorithm. I would also encourage the authors to take another look at the dynamics of the wetting front reflection for a source of additional information.

The authors are uncertain on the reviewer's use of 'much more of the information actually contained in the dataset'. The reviewer mentions analysis of the air wave and groundwave in the data. However, the airwave contains absolutely no information regarding the infiltration process. The groundwave cannot be used in reflection tomography because it is not a reflected arrival, but a direct arrival. Analysis of the groundwave analysis could be included in future efforts but would only help to constrain the results in the upper ~0.10 m of the inversion, thus it is not clear how that suggestion is particularly helpful.

We again agree with Reviewer #3 that there is indeed much potential for future studies advancing and refining algorithms for time-lapse reflection tomography, but once again we emphasize that this was not the goal that we have identified for this manuscript and well beyond the scope of work here.

For getting better results by adapting the currently employed algorithm, an approach could be to constrain the inversion based on CMPs acquired at a specific time by the results from previous and subsequent time steps. Basically: If timelapse movies helped in visual interpretation of the dataset –there is no reason to expect that this will not also be the case for an automated evaluation...

In my opinion, the fundamental limitation in the case presented here is not so much in the information content of the data set in itself (as stated in L.205), but in the limitations of the algorithm which would have to be discussed in a lot more detail in this paper to warrant a publication. The author's claim that "automated high-speed GPR data acquisition coupled with reflection tomography algorithms can provide a new approach to hydrologic monitoring" – will only hold if these algorithms actually leverage the additional information contained in the temporal domain. As far as I understood the author's approach, for each example shown, the pertaining spatially distributed series of CMPs is inverted without taking into account the information obtained at different times. Maybe each inversion is actually starting from a different starting model – but to what extent this is actually the case is not clear to me from the paper and would warrant a whole discussion of its own, e.g.: how does the starting model evolve over the time series? How much does the final inverted velocity model differ from the respective starting model? Could the starting model be in some clever way constraint by results from a previous – or in an iterative approach even a subsequent – timestep? How dense would the temporal resolution have to be for such an approach to work (btw. – the inversion seems to be quite computationally intensive, which should also be discussed in terms of potential limitations: how dense could such a temporal sampling from a computational point of view actually be?



The authors explicitly mention how the starting models were derived for the tomography algorithm (lines 87-88). In Figure 1 of this response, we show the starting models derived from semblance analysis of the simulations. We have replaced Figure 3 in the manuscript with this figure and edited the appropriate references in order to show the initial models for the tomography algorithm.

Again, we agree that there is potential for developing new algorithms for the inversion of time-lapse reflection tomography data and we are (of course) working on developing these tools, though again we emphasize that they currently do not exist.

In conclusion, so far I do not see enough evidence in the paper presented here to sustain the author's main claim that "reflection tomography in the post-migrated domain is a viable method for resolving transient soil moisture content in 2D".

Hence, which way forward? I do see two possible roads to follow:

- *Since the main claim can so far not be sustained, the only reason for publishing this paper would be to provide a much more thorough performance assessment of the employed algorithm under such dynamic infiltration conditions. Hence, radically refocus the publication to concentrate on assessing the true capabilities of the present algorithm under dynamic conditions based on (potentially a series of additional) numerical simulations – including some sort of time-lapse analysis /movies etc. as hinted at above. Improve on constraining the starting model and discuss in the framework of a rigorous error assessment. As stated above: Deriving average water content error is just a small part of the task if this is to be useful for studying dynamic cases. Correctly resolving the position of infiltration-induced interfaces over time is another. Water balance would be yet another – e.g., to what extent is the total amount of infiltrated water actually retrieved?*
- *Otherwise I would advice to keep this publication as is in the status of a discussion paper and focus the efforts on a larger inversion framework in which the present results can be one source of*

information, to be augmented by evaluating different aspects of the dataset. Please leverage much more of the information contained in the temporal nature of this great dataset. In light of my rather substantial objections to publishing the current manuscript, I will not continue adding additional minor comments at this point.

The authors respectfully disagree with the reviewer based on all of the previous replies above and the fact that three other reviews did not agree with the conclusions of this reviewer. By keeping this publication “in the status of a discussion paper” it seems that the reviewer is suggesting that the content here should remain available to the scientific community. If this is the case, then even this reviewer does indeed see value in having our work available to the public and reinforces the fact that this work should indeed be published.

Works Cited

- Busch, S., J. van der Kruk & H. Vereecken, 2014. Improved characterization of fine texture soils using onground GPS full-waveform inversion. *Transactions on Geoscience and Remote Sensing*, 52(7), pp.3947–3958.
- Ernst, J.R., H. Maurer, A.G. Green & K. Holliger, 2007. Full-Waveform Inversion of Crosshole Radar Data Based on 2-D Finite-Difference Time-Domain Solutions of Maxwell ' s Equations. *IEEE Transactions on Geoscience and Remote Sensing*, 45(9), pp.2807–2828.
- Lavoué, F., R. Brossier, L. Métivier, S. Garambois & J. Virieux, 2014. Two-dimensional permittivity and conductivity imaging by full waveform inversion of multioffset GPR data: A frequency-domain quasi-Newton approach. *Geophysical Journal International*, 197(1), pp.248–268.
- Meles, G.A., J. Van Der Kruk, S.A. Greenhalgh, J.R. Ernst, H. Maurer & A.G. Green, 2010. A new vector waveform inversion algorithm for simultaneous updating of conductivity and permittivity parameters from combination crosshole/borehole-to- surface GPR data. *IEEE Transactions on Geoscience and Remote Sensing*, 48(9), pp.3391–3407.
- Moysey, S., and R. Knight. 2004. “Modeling the Field-Scale Relationship between Dielectric Constant and Water Content in Heterogeneous Systems.” *Water Resources Research* 40(3).

1 Reflection tomography of time-lapse GPR data for studying 2 dynamic unsaturated flow phenomena

3 Adam R. Mangel^{1,2}, Stephen M.J. Moysey², John Bradford¹

4 ¹ Department of Geophysics, Colorado School of Mines, Golden, Colorado, 80401, USA

5 ² Department of Environmental Engineering and Earth Science, Clemson University, Clemson, South Carolina, 29634,
6 USA

7 *Corresponding to:* Adam R. Mangel (amangel@mines.edu)

9 Abstract

10 Ground-penetrating radar (GPR) reflection tomography algorithms allow non-invasive monitoring of water content
11 changes resulting from flow in the vadose zone. The approach requires multi-offset GPR data that is traditionally
12 slow to collect. We automate GPR data collection to reduce the survey time significantly, thereby making this
13 approach to hydrologic monitoring feasible. The method was evaluated using numerical simulations and laboratory
14 experiments that suggest reflection tomography can provide water content estimates to within 5-10% vol./vol. for the
15 synthetic studies, whereas the empirical estimates were typically within 5-15% of measurements from in-situ probes.
16 Both studies show larger observed errors in water content near the periphery of the wetting front, beyond which
17 additional reflectors were not present to provide data coverage. Overall, coupling automated GPR data collection with
18 reflection tomography provides a new method for informing models of subsurface hydrologic processes and a new
19 method for determining transient 2D soil moisture distributions.

20 1. Introduction

21 Preferential flow is ubiquitous in the vadose zone, occurring under a wide variety of conditions and over a
22 broad range of scales (Nimmo, 2012). Reviews such as those by Hendrickx and Flury (2001) and Jarvis (2007)
23 illustrate that a basic mechanistic understanding of preferential flow exists. Jarvis et al. (2016) point out, however,
24 that we still lack models capable of reproducing empirical observations in the field and highlight the importance of
25 non-invasive imaging techniques for improving this understanding. We suggest that ground-penetrating radar (GPR)
26 reflection tomography could fill this need by quantitatively mapping changes in water content through space and time
27 at the sub-meter scale.

28 Reflection GPR is commonly used to image subsurface structures, but is also well suited to understanding
29 hydrologic variability due to the strong dependence of EM wave velocities on soil volumetric water content (Topp et
30 al., 1980). As a result, GPR has been adapted to monitor variability in hydrologic processes at multiple scales through
31 time and space in a variety of contexts (Buchner et al., 2011; Busch et al., 2013; Guo et al., 2014; Haarder et al., 2011;
32 Lunt et al., 2005; Mangel et al., 2012, 2015b, 2017; Moysey, 2010; Saintenoy et al., 2007; Steelman and Endres, 2010;
33 Vellidis et al., 1990). Note that GPR methods are not applicable in media with relatively high electrical conductivity.

34 While these studies have illustrated a variety of techniques for monitoring changes in water content within
35 the subsurface, they have generally required assumptions to constrain the interpretation, such as the use of *a priori*
36 information regarding subsurface structure (e.g., Lunt et al., 2005) or the GPR wave velocity (Haarder et al., 2011).

37 These limitations arise from the fact that GPR data are recorded as energy arriving at the receiver antenna as a function
38 of time. Inherent assumptions therefore exist in analyzing traveltime data collected with antennas separated by a fixed
39 offset because both the distance travelled by the GPR wave to a reflector and the velocity of the GPR wave are
40 unknown. It has been demonstrated that GPR data collected via a multi-offset survey can constrain both the depth to
41 a moving wetting front and the water content behind the front over the course of an infiltration event (Gerhards et al.,
42 2008; Mangel et al., 2012). The limitation of these studies, however, was that the authors assumed a 1D flow system
43 and that GPR data lacked information regarding lateral variability in soil moisture.

44 Extending multi-offset techniques (Forte and Pipan, 2017; Jaumann and Roth, 2017; Klenk et al., 2015;
45 Lambot et al., 2004, 2009) to image flow in the vadose zone requires an increase in the speed at which these data can
46 be collected and advanced processing methods that can combine thousands of measurements into spatially and
47 temporally variable water content estimates. We have recently overcome the data collection problem by automating
48 GPR data collection using a computer controlled gantry, thereby reducing the data collection time for large multi-
49 offset surveys from hours to minutes (Mangel et al., 2015a). Tomography and wave migration algorithms from
50 seismic literature have been available for decades (Baysal et al., 1983; Lafond and Levander, 1993; Sava and Biondi,
51 2004a, 2004b; Stork, 1992; Yilmaz and Chambers, 1984) and are being continually adapted to GPR applications. For
52 example, this work is made possible due to adaptation of the pre-stack migration algorithm (Leparoux et al., 2001)
53 and adaptation of the reflection tomography algorithm (Bradford, 2006) to multi-offset GPR data. Subsequent studies
54 have demonstrated the use of GPR reflection tomography for imaging static distributions of subsurface water content
55 with great detail (Bradford, 2008; Bradford et al., 2009; Brosten et al., 2009). The combination of automated GPR
56 data collection and reflection tomography makes time-lapse imaging of water content during infiltration a feasible
57 means to study flow in the vadose zone.

58 The objective of this study is to evaluate reflection tomography of high-resolution GPR data as a tool for
59 observing and characterizing unsaturated flow patterns during infiltration into a homogeneous soil. To evaluate the
60 efficacy of the algorithm for resolving dynamic soil water content in 2D, we first test the algorithm using numerical
61 simulations and compare the results to true water content distributions. We then apply the algorithm to time-lapse
62 GPR data collected during an infiltration and recovery event in a homogeneous soil and compare results to
63 measurements from in-situ soil moisture probes.

64 **2. Methods**

65 **2.1. The Reflection Tomography Algorithm**

66 The goal of reflection tomography is to determine a velocity model that best aligns migrated reflection
67 arrivals for a common reflection point across a set of source-receiver offsets. For brevity, we will limit our discussion
68 here to the key ideas and methods of the tomography algorithm; we refer the reader to Stork (1992) for the original
69 tomography algorithm and to Bradford (2006) for the application to GPR data.

70 The data required for this algorithm are an ensemble of common-midpoint (CMP) gathers collected along a
71 path. Given that GPR data is a time-series record of electromagnetic energy arriving at a point in space, we must
72 know the proper velocity structure to migrate the data and produce a depth registered image of the GPR energy.
73 Migration attempts to remove the hyperbolic trend of reflections with respect to antenna offset (Figure 1a) by using

74 the wave velocity to reposition reflections to the proper depth at which they occur. If CMP data are migrated with the
75 correct velocity, reflections from layers in the subsurface are flattened as a function of offset (Fig. 1c). If the velocity
76 estimate is incorrect, e.g. 10% too slow (Fig. 1b) or 10% too fast (Fig. 1d), the arrival is not flat and exhibits residual
77 moveout (RMO). To solve for the velocity structure and properly migrate the data, the reflection tomography
78 algorithm proceeds as follows (Bradford, 2006; Stork, 1992):

- 79 1. Generate a starting depth vs. velocity model.
- 80 2. Migrate the data with the starting velocity model and stack the data.
- 81 3. Pick horizons on the stacked image.
- 82 4. Perform ray-tracing to the picked horizons with the velocity model.
- 83 5. Evaluate horizons for residual moveout.
- 84 6. Adjust velocity model using reflection tomography.
- 85 7. Apply revised velocity model using migration and quality check RMO.
- 86 8. Iterate at step three if necessary.

87 For this work, starting velocity models for the tomography algorithm are determined by smoothing results
88 from 1D velocity analysis of individual CMPs (Neidell and Taner, 1971). The reflection tomography algorithm then
89 adjusts the velocity distribution until reflections in the depth corrected (i.e., migrated) data line up to produce a
90 reflection at a consistent depth across all traces in a CMP. Through sequential iterations of the tomographic inversion,
91 the RMO metric is reduced on a global scale. For this work, the reflection tomography was performed using the
92 SeisWorks software suite and Kirchhoff pre-stack depth migration (Yilmaz and Doherty, 2001).

93 2.2. Experimental Setup and Procedure

94 We used a 4 m x 4 m x 2 m tank for the controlled study of unsaturated flow phenomenon with GPR (Fig.
95 1e, f). We filled the tank with a medium-grained sand to a depth of 0.60 m. Below the sand was a 0.30 m layer of
96 gravel that acts as backfill for 16 individual drain cells that are pitched slightly toward central drains that route water
97 to outlets on the outside of the tank. We constructed an automated data collection system to allow for the high-speed
98 high-resolution collection of GPR data (Mangel et al., 2015a); the GPR gantry fits inside of the tank so the antennas
99 are in contact with the sand surface. All GPR data described here were collected along the y-axis of the tank at a fixed
100 position of $x = 2.0$ m, where the bottom of the tank is flat (Fig. 1e, f).

101 The automated system, which utilizes a 1000 MHz Sensors and Software bistatic radar (Sensors and
102 Software, Inc.), was operated to obtain 101 CMPs spaced at 0.02 m intervals between $y = 1.0 - 3.0$ m. Each CMP
103 consisted of 84 traces with offsets between 0.16-1.0 m at 0.01 m step size. Thus, a complete CMP data set for one
104 observation time consists of almost 8,500 individual GPR traces. With this configuration using the automated system,
105 a CMP at a single location could be collected in 1.8 seconds with a total cycle of CMP data locations collected every
106 3.9 minutes.

107 GPR data collection occurred prior to irrigation to evaluate background conditions. Data collection continued
108 during irrigation, which was applied at a flux of 0.125 cm/min for a duration of 2.13 hrs. Spatial heterogeneity in the
109 applied flux has been observed in laboratory testing of the irrigation equipment. Fifteen EC-5 soil moisture probes
110 (METER, Inc.) logged volumetric water content at 10 second intervals during the experiment (Fig. 1e, f). Note that

111 the soil moisture probes are located out of the plane of the GPR line by 0.5 m (Figure 1f). GPR data collection
112 continued for 40 min. after the irrigation was terminated. In total, 45 complete sets of data were collected over the
113 course of the 3-hour experiment, yielding more than 500,000 GPR traces in the experimental data set.

114 2.3. Execution of the Numerical Simulations

115 We employed HYDRUS-2D (Simunek and van Genuchten, 2005) to simulate a theoretical and realistic
116 hydrologic response to an infiltration event using two different initial conditions: i) hydrostatic equilibrium leading to
117 a water content distribution controlled by the soil water retention curve, and ii) a uniform soil with a water content of
118 0.07. We selected the Mualem-van Genuchten soil model (Mualem, 1976) and parameterized the model as follows
119 based on hydraulic testing of the sand: residual water content (θ_r) = 0.06, saturated water content (θ_s) = 0.38, air-entry
120 pressure (α) = 0.058 cm⁻¹, shape parameter (n) = 4.09, and saturated hydraulic conductivity (K_s) = 4.6 cm min⁻¹. The
121 hydraulic conductivity for the homogeneous model was reduced to 1 cm min⁻¹ to build a larger contrast of water
122 content across the wetting front. For all HYDRUS simulations, we used a constant flux boundary condition of 0.125
123 cm/min from $y = 1.6 - 2.4$ m along the ground surface, set the model domain depth to 0.6 m, length to 4.0 m, and
124 nominal cell size to 0.04 m. Remaining nodes at the surface were set to no flow boundaries and lower boundary nodes
125 were set to a seepage face with the pressure head equal to zero.

126 We calculated relative dielectric permittivity values for the GPR simulations by transforming water content values
127 from HYDRUS-2D using the Topp equation (Topp et al., 1980). We used the magnetic permeability of free space for
128 the entire model domain and set electrical conductivity of the soil to 1 mS/m. Although electrical conductivity changes
129 as a function of the water content, these changes primarily influence wave attenuation, which is not significant or
130 accounted for in the processing performed with the SeisWorks software.

131 We performed GPR simulations in MATLAB using a 2D finite-difference time-domain code (Irving and
132 Knight, 2006). The GPR model domain was set to 4.0 m long and 1.1 m high with a cell size of 0.002 m. The lower
133 0.3 m of the domain was set to a relative dielectric permittivity of 2.25 to represent the lower gravel layer and the
134 upper 0.2 m was modeled as air to simulate the air-soil interface. Simulated data were collected as described in the
135 section detailing the tank experiment. For quick computation, simulations were deployed on the Palmetto
136 supercomputer cluster at Clemson University, where single source simulations ran in 20 minutes using nodes with 8
137 CPUs and 32 GB of RAM.

138 3. Reflection Tomography of Simulations

139 The HYDRUS-2D output shows the development of an infiltrating wetting front for the two scenarios with
140 differing initial conditions (Figs. 2a, f, k). For conditions prior to irrigation, the bottom of sand reflection (B) is
141 horizontal on the common-offset profile (COP) data indicating a constant velocity across the model domain (Fig. 2b).
142 Additionally, the CMPs show identical hyperbolic moveout, i.e., the offset vs. travelttime relationship, indicating a
143 homogeneous velocity across the model domain (Fig. 2c-e). The airwave and groundwave are also visible in the data,
144 but are not analyzed, or further discussed.

145 During infiltration, (B) is distorted at the center of the COP due to the decreased velocity caused by the
146 infiltrating water (Figs. 2g, l). A reflection from the infiltrating wetting front (W) is faintly visible for the model with
147 variable initial water contents (Fig. 2g) and comparatively strong for simulations with a dry background (Fig. 2l) due

148 to different levels of dielectric contrast across the wetting front in each case. CMPs also indicate perturbations in the
149 velocity field as the moveout changes dramatically when the wetted zone is encountered (Figs. 2h-j, m-o). A refraction
150 is also observed on the CMPs, which is a rare occurrence considering that GPR wave velocity typically decreases with
151 depth.

152 Prior to the onset of flow, the reflection tomography algorithm produces a uniform water content distribution
153 that agrees with the arithmetic average of the true water content but does not capture the vertical gradation observed
154 in Figure 3a. This is because information regarding vertical velocity variations is absent, i.e., more reflectors at
155 different depths are required to capture this variability. As a result, errors in the water content estimation exceed 10%
156 vol./vol (Fig. 3de).

157 During infiltration the wetting front is imaged relatively well for the case where the soil was initially dry
158 (Figs. 3g-i-l), particularly as the plume advances deeper into the subsurface (Figs. 3j-m-p) where there is improved
159 data coverage. The tomography algorithm overestimates the depth of the wetting front by roughly 0.10 m for the case
160 presented in Figure 3i-l, which is likely due to smoothing effects required to regularize the inversion or an error in the
161 picking of the wetting front horizon. Considerable errors in the tomography results persist, however, with the results
162 degrading further for the scenario with variable initial water content (Figs. 3d-fe-h) given that reflection contrasts with
163 the wetting front are weaker. The presence of an additional reflector, however, increases the ability of the tomography
164 to resolve vertical variability, e.g. Figure 2e-2g vs. Figure 2b. Overall, errors are reduced near reflectors to about 5%
165 vol./vol. These results suggest that water content changes resulting from unsaturated flow can be imaged and that as
166 more information becomes available in the form of additional reflections, the tomography results improve.

167 4. Reflection Tomography of Experimental Data

168 At initial conditions, the sand layer reflection (B) is visible at 10 ns traveltimes in the COP collected over the
169 imaging area (Fig. 4a). Normal hyperbolic moveout of (B) is observed on the CMPs (Fig.4b, c, d). These results are
170 qualitatively identical to observations from numerical simulations (Figs. 2b-e).

171 During infiltration, the water content of the sand layer increases substantially (Fig. 5) and longer traveltimes
172 of the arrivals on the COP data are observed near the center of the tank (Figs. 4f, i). Rather than a coherent reflection
173 for the wetting front (W) (Fig. 2l), multiple discrete reflections are present in the COP data (Fig. 4e, i, m) indicating
174 a heterogeneous wetting of the soil. These reflections are difficult to identify on the CMPs given the complex moveout
175 pattern (Fig. 4i) but are more easily identified in animations of COP projections of the data (included as a
176 supplementary file). Analysis of the data was greatly aided by the animation of the data and the pre-stack migration
177 algorithm, which stacks the data over all offsets to produce a coherent image of reflectors with an increased signal to
178 noise ratio. Heterogeneous wetting of the soil is also very pronounced in the soil-moisture probe data with many of
179 the probes responding out of sequence with depth (Fig 5). After irrigation, the soil moisture probes show a decrease
180 in the soil water content (Fig. 5) apart from one probe (Fig. 5c) and the GPR data show a slight decrease in the
181 traveltimes of the bottom of sand reflection (Figs. 4k-n).

182 The tomographic imaging results from the initial GPR data set collected prior to irrigation agree with data
183 from soil moisture probes which indicates an average soil moisture of roughly 5% during this time (Figs. 4e, 5).
184 During infiltration and recovery, tomographic images of the tank show a wet zone at the center and relatively dry

185 edges outside the irrigated area (Figs. 4j, o). Overall, the tomography results near the center of the tank are within
186 10% vol./vol. of the soil moisture data and show a non-uniform wetting of the soil during infiltration that was not
187 observed in the numerical study, suggesting the occurrence of preferential flow. Errors in the estimates of water
188 content near the edges of the advancing plume exceed 15% vol./vol. (Fig. 4b, c), though the general patterns in wetting
189 are consistent. After irrigation, the tomography results on the edges of the wetted zone are in better agreement with
190 the soil moisture probe data, but less spatial information is available given the lack of a wetting front reflection (Fig.
191 4o).

192 5. Conclusions

193 Reflection tomography in the post-migrated domain is a viable method for resolving transient soil moisture
194 content in 2D associated with an infiltration and recovery event in a homogeneous soil. Reflection tomography of
195 numerical data produced water content distributions that were in good agreement with true water content values from
196 the simulations. The tomography was generally able to match the true water content values to within 5-10% vol./vol.
197 However, distinct migration artifacts were produced around the edges of the wetting front, especially for cases where
198 the initial water content was non-uniform, obscuring details about the shape of the wetted region. Analysis of data
199 collected in a sand tank proved to be more difficult, however, the tomography was able to produce hydrologically
200 realistic distributions of water content in space and time that were generally within 5-15% vol./vol. of measurements
201 from in-situ soil moisture probes. This may have to do with the complex distribution of the wetted soil as a result of
202 heterogenous distribution of water at the surface, texture variability in the soil, or other preferential flow mechanisms
203 (Jarvis et al., 2016). Regardless, the fact that the GPR data were able to capture this heterogeneity is an impressive
204 feat given that tomographic imaging operated independently of any hydrologic information and provided evidence
205 that our conceptual model was not representative of the physical system.

206 Regardless of discrepancies observed between the GPR and probe water content values, it is evident that
207 automated high-speed GPR data acquisition coupled with reflection tomography algorithms can provide a new
208 approach to hydrologic monitoring. Testing and revision of conceptual hydrologic models regarding non-uniform
209 flow in the vadose zone demands such non-invasive time-lapse imaging data. Artifacts observed in the numerical
210 simulation results, however, suggest that improvements in this methodology could be achieved. While there are likely
211 fundamental limitations to the information content of the data, the Kirchhoff pre-stack depth migration algorithm used
212 in this study could be replaced by more sophisticated algorithms like reverse-time migration (Baysal et al., 1983)
213 which may reduce the observed imaging artifacts. Additionally, results from the tomography algorithm may prove to
214 be beneficial as a precursor to higher-order inversion techniques, like full-waveform inversion, which requires detailed
215 starting models of velocity for convergence. Overall, coupling automated GPR data collection with reflection
216 tomography provides a new method for informing models of subsurface hydrologic processes and a new method for
217 determining transient 2D soil moisture distributions.

218 6. Acknowledgements

219 This material is based upon work supported by, or in part by, the National Science Foundation under grant
220 number EAR-1151294. We also acknowledge Clemson University for generous allotment of compute time on

221 Palmetto cluster. Data used in this publication and a supplementary movie of the data are available through the
222 Colorado School of Mines at the following URL: <https://hdl.handle.net/11124/172053>.

223 7. References

- 224 Baysal, E., Kosloff, D. and Sherwood, J.: Reverse Time Migration, *Geophysics*, 48(11), 1514–1524,
225 doi:10.1190/1.1441434, 1983.
- 226 Bradford, J. H.: Applying reflection tomography in the postmigrated domain to multifold ground-penetrating radar
227 data, *Geophysics*, 71(1), K1–K8, doi:10.1190/1.2159051, 2006.
- 228 Bradford, J. H.: Measuring Water Content Heterogeneity Using Multifold GPR with Reflection Tomography, *Vadose*
229 *Zo. J.*, 7(1), 184, doi:10.2136/vzj2006.0160, 2008.
- 230 Bradford, J. H., Clement, W. P. and Barrash, W.: Estimating porosity with ground-penetrating radar reflection
231 tomography: A controlled 3-D experiment at the Boise Hydrogeophysical Research Site, *Water Resour. Res.*, 45(4),
232 n/a-n/a, doi:10.1029/2008WR006960, 2009.
- 233 Brosten, T. R., Bradford, J. H., McNamara, J. P., Gooseff, M. N., Zarnetske, J. P., Bowden, W. B. and Johnston, M.
234 E.: Multi-offset GPR methods for hyporheic zone investigations, *Near Surf. Geophys.*, 7, 244–257, 2009.
- 235 Buchner, J. S., Kuhne, A., Antz, B., Roth, K. and Wollschläger, U.: Observation of volumetric water content and
236 reflector depth with multichannel ground-penetrating radar in an artificial sand volume, 2011 6th Int. Work. Adv. Gr.
237 Penetrating Radar, 1–5, doi:10.1109/IWAGPR.2011.5963910, 2011.
- 238 Busch, S., Weihermüller, L., Huisman, J. A., Steelman, C. M., Endres, A. L., Vereecken, H. and van der Kruk, J.:
239 Coupled hydrogeophysical inversion of time-lapse surface GPR data to estimate hydraulic properties of a layered
240 subsurface, *Water Resour. Res.*, 49(12), 8480–8494, doi:10.1002/2013WR013992, 2013.
- 241 Forte, E. and Pipan, M.: Review of multi-offset GPR applications: Data acquisition, processing and analysis, *Signal*
242 *Processing*, 132, 1–11, doi:10.1016/j.sigpro.2016.04.011, 2017.
- 243 Gerhards, H., Wollschläger, U., Yu, Q., Schiwek, P., Pan, X. and Roth, K.: Continuous and simultaneous
244 measurement of reflector depth and average soil-water content with multichannel ground-penetrating radar,
245 *Geophysics*, 73(4), 15–23, 2008.
- 246 Gloaguen, E., Chouteau, M., Marcotte, D. and Chapuis, R.: Estimation of hydraulic conductivity of an unconfined
247 aquifer using cokriging of GPR and hydrostratigraphic data, *J. Appl. Geophys.*, 47(2), 135–152, doi:10.1016/S0926-
248 9851(01)00057-X, 2001.
- 249 Guo, L., Chen, J. and Lin, H.: Subsurface lateral preferential flow network revealed by time-lapse ground-penetrating
250 radar in a hillslope, *Water Resour. Res.*, 50, 9127–9147, doi:10.1002/2013WR014603, 2014.
- 251 Haarder, E. B., Looms, M. C., Jensen, K. H. and Nielsen, L.: Visualizing Unsaturated Flow Phenomena Using High-
252 Resolution Reflection Ground Penetrating Radar, *Vadose Zo. J.*, 10(1), 84, doi:10.2136/vzj2009.0188, 2011.
- 253 Hendrickx, J. M. H. and Flury, M.: Uniform and Preferential Flow Mechanisms in the Vadose Zone, in *Conceptual*
254 *Models of Flow and Transport in the Fractured Vadose Zone*, pp. 149–187, National Academy Press, Washington,
255 D.C., 2001.
- 256 Irving, J. and Knight, R.: Numerical modeling of ground-penetrating radar in 2-D using MATLAB, *Comput. Geosci.*,
257 32(9), 1247–1258, doi:10.1016/j.cageo.2005.11.006, 2006.

258 Jarvis, N., Koestel, J. and Larsbo, M.: Understanding Preferential Flow in the Vadose Zone: Recent Advances and
259 Future Prospects, *Vadose Zo. J.*, 15(12), 0, doi:10.2136/vzj2016.09.0075, 2016.

260 Jarvis, N. J.: A review of non-equilibrium water flow and solute transport in soil macropores: Principles, controlling
261 factors and consequences for water quality, *Eur. J. Soil Sci.*, 58(3), 523–546, doi:10.1111/j.1365-2389.2007.00915.x,
262 2007.

263 Jaumann, S. and Roth, K.: Soil hydraulic material properties and subsurface architecture from time-lapse GPR,
264 *Hydrol. Earth Syst. Sci. Discuss.*, (September), 1–34, doi:10.5194/hess-2017-538, 2017.

265 Klenk, P., Jaumann, S. and Roth, K.: Quantitative high-resolution observations of soil water dynamics in a complicated
266 architecture using time-lapse ground-penetrating radar, *Hydrol. Earth Syst. Sci.*, 19(3), 1125–1139, doi:10.5194/hess-
267 19-1125-2015, 2015.

268 Lafond, C. F. and Levander, A. R.: Migration moveout analysis and depth focusing, *Geophysics*, 58(1), 91–100,
269 doi:10.1190/1.1443354, 1993.

270 Lambot, S., Antoine, M., van den Bosch, I., Slob, E. C. and Vanclooster, M.: Electromagnetic Inversion of GPR
271 Signals and Subsequent Hydrodynamic Inversion to Estimate Effective Vadose Zone Hydraulic Properties, *Vadose*
272 *Zo. J.*, 3(4), 1072, doi:10.2136/vzj2004.1072, 2004.

273 Lambot, S., Slob, E., Rhebergen, J., Lopera, O., Jadoon, K. Z. and Vereecken, H.: Remote Estimation of the Hydraulic
274 Properties of a Sand Using Full-Waveform Integrated Hydrogeophysical Inversion of Time-Lapse, Off-Ground GPR
275 Data, *Vadose Zo. J.*, 8(3), 743, doi:10.2136/vzj2008.0058, 2009.

276 Leparoux, D., Gibert, D. and Cote, P.: Adaptation of prestack migration to multi-offset ground-penetrating radar
277 (GPR) data, *Geophys. Prospect.*, 49(3), 374–386, doi:10.1046/j.1365-2478.2001.00258.x, 2001.

278 Lunt, I. A., Hubbard, S. S. and Rubin, Y.: Soil moisture content estimation using ground-penetrating radar reflection
279 data, *J. Hydrol.*, 307(1–4), 254–269, doi:10.1016/j.jhydrol.2004.10.014, 2005.

280 Mangel, A. R., Moysey, S. M. J., Ryan, J. C. and Tarbutton, J. A.: Multi-offset ground-penetrating radar imaging of
281 a lab-scale infiltration test, *Hydrol. Earth Syst. Sci.*, 16(11), doi:10.5194/hess-16-4009-2012, 2012.

282 Mangel, A. R., Lytle, B. A. and Moysey, S. M. J.: Automated high-resolution GPR data collection for monitoring
283 dynamic hydrologic processes in two and three dimensions, *Lead. Edge*, 34(2), doi:10.1190/le34020190.1, 2015a.

284 Mangel, A. R., Moysey, S. M. J. and van der Kruk, J.: Resolving precipitation induced water content profiles by
285 inversion of dispersive GPR data: A numerical study, *J. Hydrol.*, 525, 496–505, doi:10.1016/j.jhydrol.2015.04.011,
286 2015b.

287 Mangel, A. R., Moysey, S. M. J. and van der Kruk, J.: Resolving infiltration-induced water content profiles by
288 inversion of dispersive ground-penetrating radar data, *Vadose Zo. J.*, 16, doi:10.2136/vzj2017.02.0037, 2017.

289 Moysey, S. M.: Hydrologic trajectories in transient ground-penetrating-radar reflection data, *Geophysics*, 75(4),
290 WA211-WA219, doi:10.1190/1.3463416, 2010.

291 Mualem, Y.: A new model for predicting the hydraulic conductivity of unsaturated porous media, *Water Resour. Res.*,
292 12(3), 1976.

293 Neidell, N. S. and Taner, M. T.: Semblance and other coherency measures for multichannel data, *Geophysics*, 36(3),
294 482–497, 1971.

295 Nimmo, J. R.: Preferential flow occurs in unsaturated conditions, *Hydrol. Process.*, 26(5), 786–789,
296 doi:10.1002/hyp.8380, 2012.

297 Saintenoy, A., Schneider, S. and Tcholka, P.: Evaluating GroundPenetrating Radar use for water infiltration
298 monitoring, 2007 4th Int. Work. on, Adv. Gr. Penetrating Radar, 91–95, doi:10.1109/AGPR.2007.386531, 2007.

299 Sava, P. and Biondi, B.: Wave-equation migration velocity analysis. I. Theory, *Geophys. Prospect.*, 52(6), 593–606,
300 doi:10.1111/j.1365-2478.2004.00447.x, 2004a.

301 Sava, P. and Biondi, B.: Wave-equation migration velocity analysis — II: Subsalt imaging examples *Geophysical*
302 *Prospecting*, accepted for publication, , 1–36, 2004b.

303 Simunek, J. and van Genuchten, M. T.: HYDRUS code for simulating the movement of water, heat, and multiple
304 solutes in variably saturated porous media, 2005.

305 Steelman, C. M. and Endres, A. L.: An examination of direct ground wave soil moisture monitoring over an annual
306 cycle of soil conditions, *Water Resour. Res.*, 46(11), n/a-n/a, doi:10.1029/2009WR008815, 2010.

307 Stork, C.: Reflection tomography in the postmigrated domain, *Geophysics*, 57(5), 680–692, doi:10.1190/1.1443282,
308 1992.

309 Topp, G. C., Davis, J. L. and Annan, A. P.: Electromagnetic Determination of Soil Water Content:, *Water Resour.*
310 *Res.*, 16(3), 574–582, 1980.

311 Vellidis, G., Smith, M. C., Thomas, D. L. and Asmussen, L. E.: Detecting wetting front movement in a sandy soil
312 with ground-penetrating radar, *Am. Soc. Agric. Eng.*, 33(6), 1867–1874, 1990.

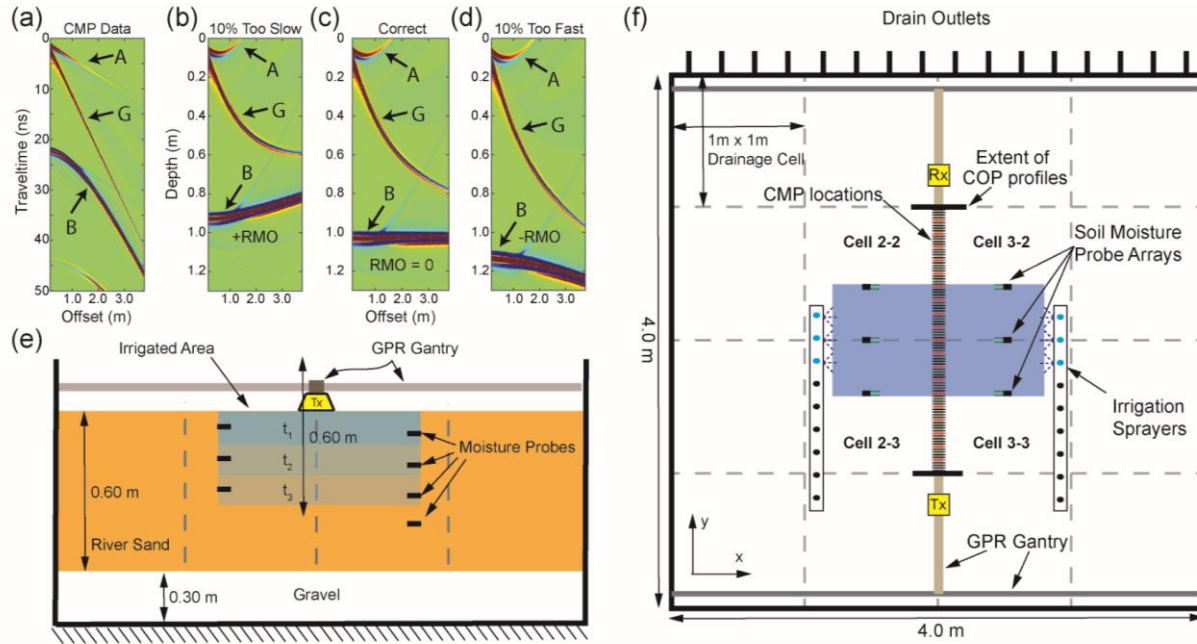
313 Yilmaz, O. and Chambers, R.: Migration velocity analysis by wave-field extrapolation, *Geophysics*, 49(10), 1664–
314 1674, 1984.

315 Yilmaz, O. and Doherty, S.: *Seismic Data Analysis: Processing, Inversion, and Interpretation of Seismic Data*, 2nd
316 ed., Society of Exploration Geophysicists, Tulsa, OK., 2001.

317

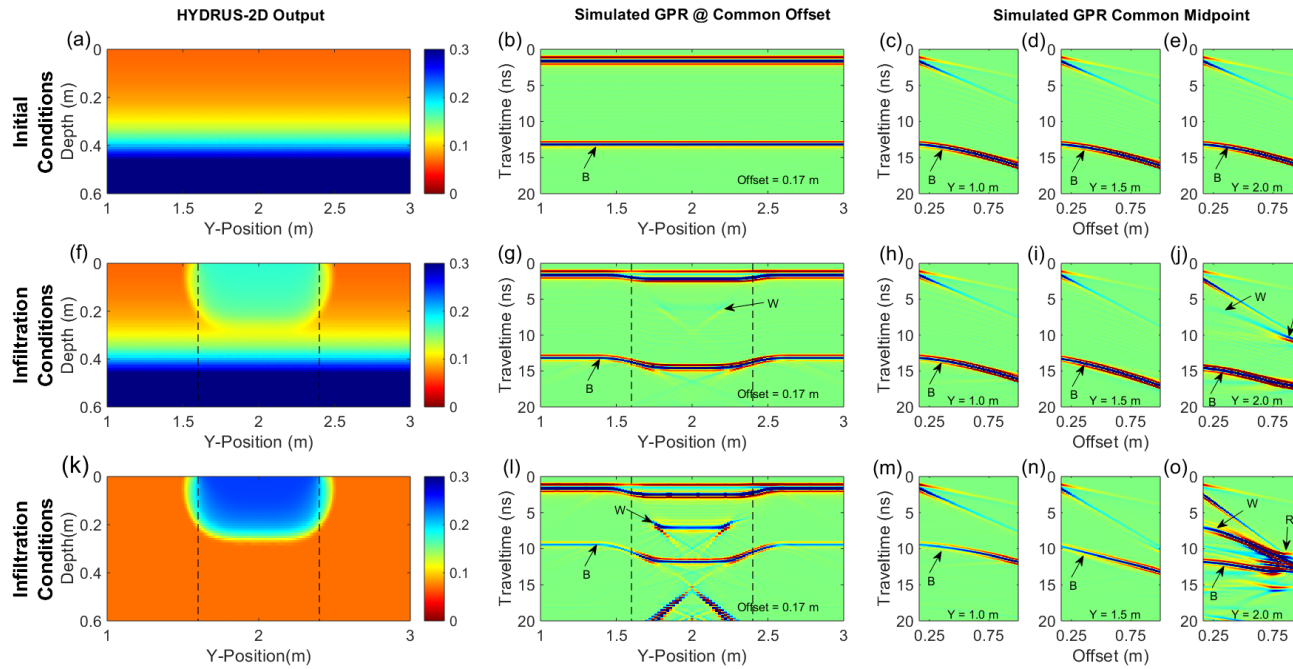
318 8. Figures

319 Figure 1



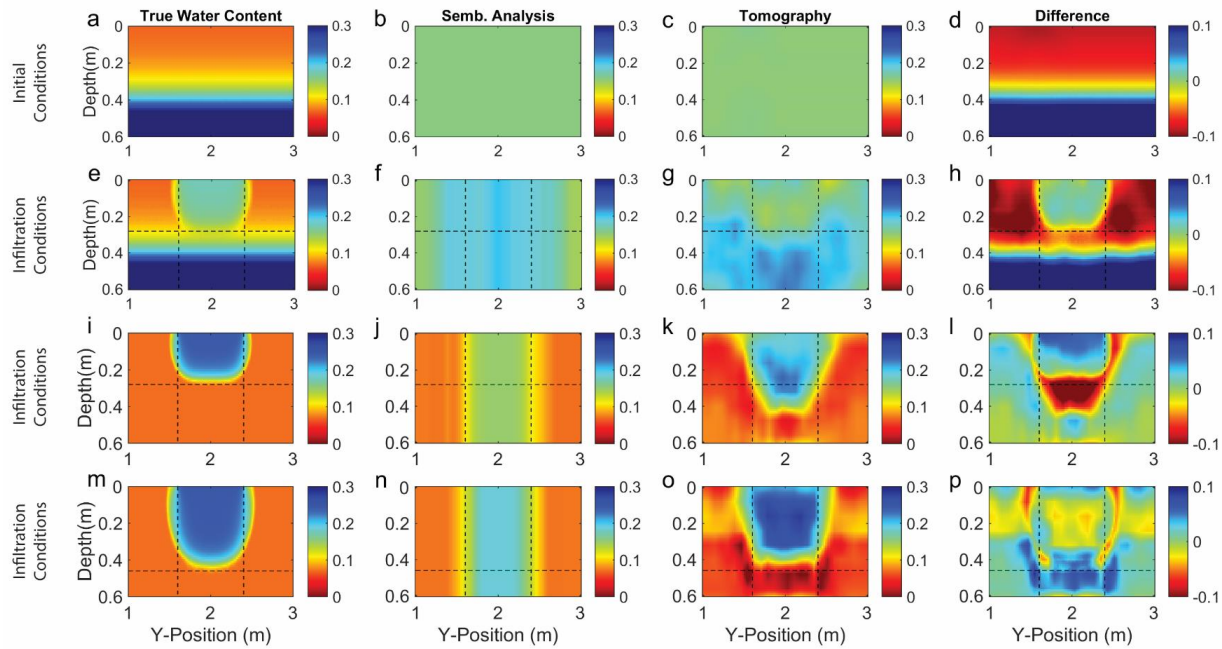
320

321 Figure 1: a) Example CMP data showing the airwave (A), groundwave (G) and reflection from a layer (B). Data in (a) is migrated to form (b) a migrated gather
 322 with velocity 10% slow; (c) a migrated gather with correct velocity; and (d) a migrated gather with velocity 10% fast. Panel (e) shows a cross-section of the experiment
 323 at $y = 2.0$ where t_1 , t_2 , and t_3 are arbitrary times during the infiltration. Panel (f) shows the plan-view of the experiment. Note that the bottom of the sand layer is
 324 flat where GPR data collection occurs, i.e. on a boundary between drain cells, and pitched elsewhere toward cell drains.



326
 327 Figure 2: Panels (a), (f), and (k) show volumetric moisture distribution from HYDRUS-2D simulations used to generate simulated common-offset GPR data (b, g,
 328 l) and multi-offset GPR data (c-e, h-j, and m-o). Vertical dashed lines indicate the extent of the wetted surface. Annotated arrivals are the bottom of sand layer
 329 reflection (B), wetting front reflection (W), and refraction (R). Note that the base of sand reflection (B) is caused by the boundary at 0.60 m depth between the sand
 330 and gravel, not the capillary rise shown in panels (a) and (f).

331 **Figure 3**

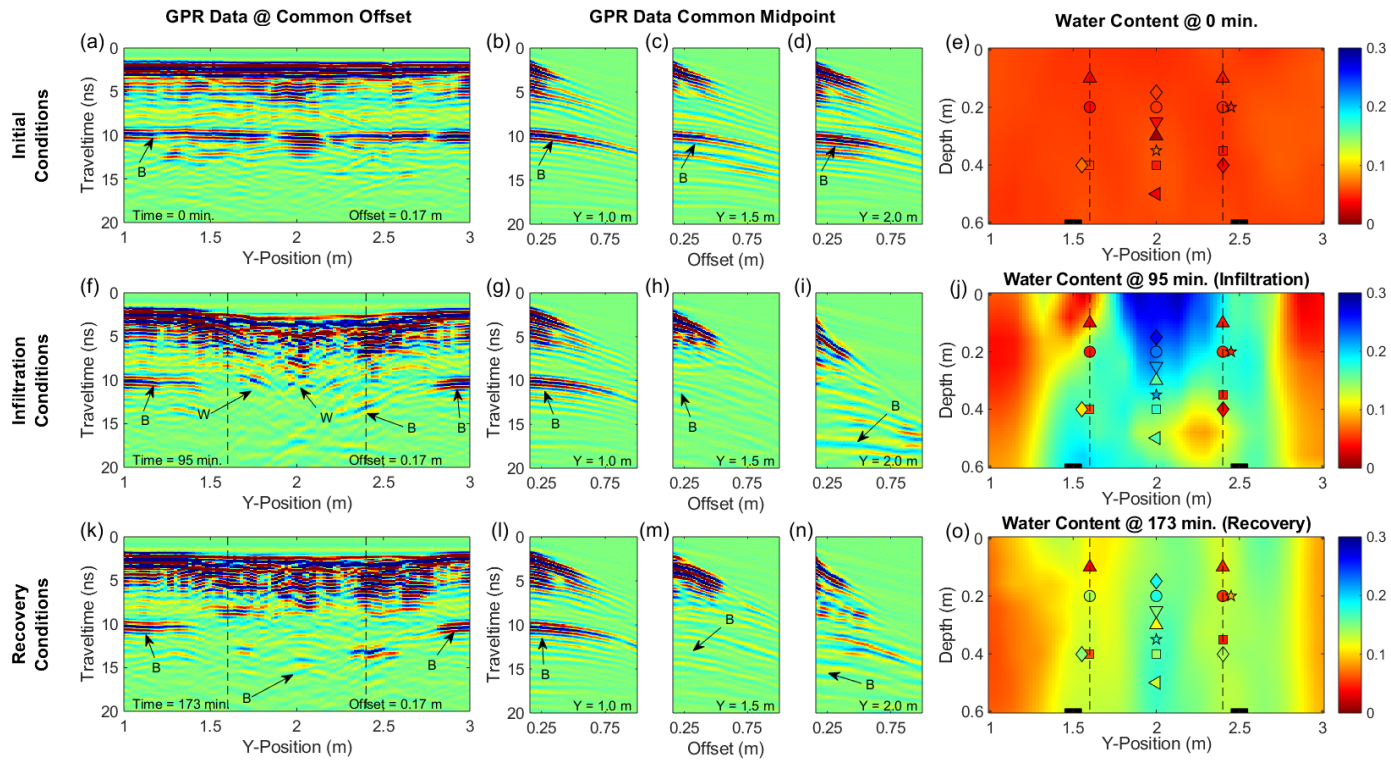


332

333 Figure 3: Panels (a), (e), (i), and (m) show true volumetric water content distributions from HYDRUS-2D. Panels (b), (f), (j), and (n) show starting models for
334 the tomography derived from semblance analysis. Panels (c), (g), (k), and (o) show results of tomography of the simulated GPR data as volumetric water
335 content. Difference plots (d), (h), (l), and (p) were calculated by subtracting the tomography results from the true water content distributions; red areas indicate
336 volumetric moisture underestimation-overestimation while blue areas indicate volumetric moisture overestimation-underestimation.

337

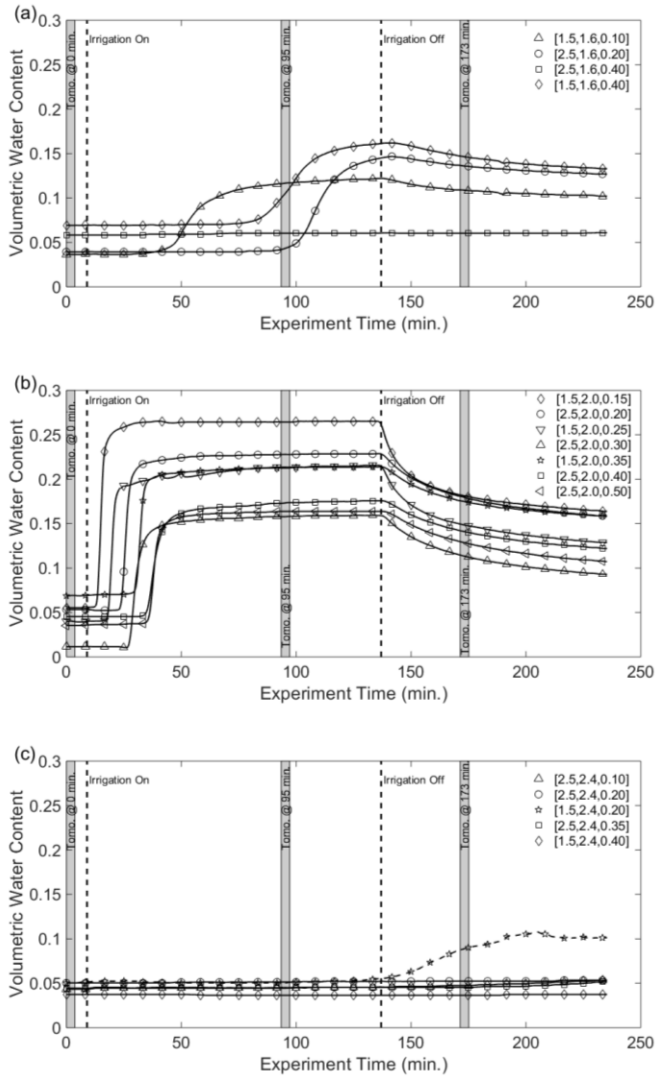
Formatted: Centered



339

340 Figure 4: Panels (a, f, and k) are common-offset GPR data collected during the experiment. Panels (b-d, g-i, and l-n) are CMP data collected during the experiment.
 341 Arrivals annotated are the sand layer reflection (B) and wetting front reflection (W). Panels (e, j, and o) show tomography results for the corresponding GPR data.
 342 Vertical lines indicate the lateral extent of the wetted surface. Shapes correspond to the soil moisture data for the given y-location in Figure 5, colors correspond to
 343 the measured soil moisture. Adjacent symbols are from probes that are located at different x-locations, but identical depths.

344 **Figure 5**



345
 346 Figure 5: Soil moisture probe data from the in-situ moisture probes along the GPR line at a) $y = 1.6$ m; b) $y = 2.0$ m;
 347 and c) $y = 2.4$ m. Vertical dashed lines indicate the start and stop of irrigation. Gray bars indicate the times when data
 348 in Figure 4 were collected. Symbols for a given data set match those on Figures 4e, j, and o. Soil moisture data were
 349 collected 60 minutes beyond the end of GPR data collection.